Interfacial Carriers Dynamics of CdS Nanoparticles

S. Logunov,† T. Green, S. Marguet,‡ and M. A. El-Sayed*

Laser Dynamics Laboratory, School of Chemistry and Biochemistry, Georgia Institute of Technology, Atlanta, Georgia 30332-0400

Received: December 2, 1997; In Final Form: February 18, 1998

The relaxation dynamics of charge carriers in 4 nm CdS colloidal quantum dots are studied by means of picosecond time-resolved fluorescence and femtosecond transient absorption experiments. We also studied the effects of the adsorption of viologen derivatives as electron acceptors on the surface of these particles. From these experimental measurements, we reached a model of the electron-hole dynamics in these nanoparticles consistent with previous proposals. In particular, we have confirmed that the electron trapping in these particles is slower than the hole trapping (30 ps versus a few picoseconds). After excitation, rapid formation of an optical hole (bleach) within the lowest energy exciton (band gap) absorption region appears. The maximum of the bleaching band is red-shifted by 20 meV in 2.5 ps, and the bleach intensity recovers in 30 ps. Upon the adsorption of electron acceptors, the rate of the red shift of the optical hole is not affected while the bleach recovery time is reduced to a few picoseconds. This leads to the following conclusions: (1) the shift in the bleach band results from hole trapping dynamics, and (2) the bleach recovery is rate limited by the electron trapping process in the CdS nanoparticles (30 ps) or by the hole trapping process (a few picoseconds) in the presence of the electron acceptors. The latter conclusion supports a previous proposal by Klimov et al., that the rate of the recovery in CdS nanoparticles is determined by the electron surface trapping process. The electron transfer to the viologen acceptors is found to be very efficient and takes place in 200−300 fs, which efficiently competes with surface trapping and electron-hole recombination processes and thus quenches both the band gap and the deep trap emissions.

Introduction

The study of exciton dynamics in CdS nanoparticles has received considerable attention in the past few years.[1−11] When the dimension of the nanocrystal becomes smaller than the de Broglie wavelength of the exciton, the quantum size effects appear; i.e., levels become discrete, and one observes a blue shift of the exciton energy and an enhancement of the absorption cross section as well as of the nonlinear optical properties.[1] When the surface-to-volume ratio becomes considerably large, the quality of the surface becomes important in determining many of the nanocrystal properties, e.g., trapping and emission.

Dynamics of the electrons and holes have been studied in several reports using different techniques, primarily transient absorption and time-resolved fluorescence.[1−11] However, it is still open to question which of the carriers (electron or hole) is trapped first. These studies have shown that excitation led to the bleach of the lowest excitonic transition in a time scale shorter than 100 fs.[12] The recovery of this bleach was found to be nonexponential, even at low excitation laser power, and had a lifetime between 30 ps and a few nanoseconds.[3,11] Two possible mechanisms were proposed for the lowest excitonic band bleach recovery.[3,11,12] The first was a band filling mechanism similar to that known to occur in bulk semiconductors which explained the transient absorption measured with 100 fs time resolution.[12] The second mechanism was related to carrier trapping at the surface states which led to a decrease in the oscillator strength of the transition due to an electrostatic interaction between a trapped electron and the hole.[3] The fact that the hole effective mass is 6 times larger than that of the electron makes it more localized than that of the electron. Thus, the electrostatic interaction between the trapped electron and the hole shifts the excitonic transition to lower energy with substantial loss in its oscillator strength.[3,11]

The fluorescence and transient absorption kinetics are extremely sensitive to surface defects.[2,4,5,9] For the 4 nm particles studied here, about 15% of the atoms are located on the surface. Three kinds of fluorescence were found for CdS nanoparticles. The first was high-energy luminescence (superradiant luminescence) due to the band gap emission, which is observed only under certain conditions (size and temperature dependent) with a lifetime of a few picoseconds.[12] The second was a near band gap emission that has a lifetime which varies between tens of picoseconds to nanoseconds and whose intensity was strongly dependent upon the conditions of the surface.[4] The third was the deep trap emission which was ∼0.9 eV red-shifted from the band gap emission and decayed in considerably longer time (up to a few microseconds under certain conditions). The ratio of the band gap to deep trap fluorescence intensities strongly depends on surface modification.

Recently, from the results of the subpicosecond transient absorption and fluorescence spectroscopy, it was proposed that the electron has slower surface trapping dynamics (30 ps) than the hole.[12] This conclusion was based on the fact that the hole has a higher density of trapping states near the edge of the valence band (VB) due to larger effective mass. To test this proposal and to study the dynamics of trapping in CdS nanoparticles, we examined the effects of surface adsorption

† Present address: Corning, Inc., Corning, NY 14831.

‡ Permanent address: Laboratoire de Photophysique et de Photochimie, DRECAM/SCM CNRS-URA 331, CEA/Saclay, F-91191 Gif-Sur-Yvette, France.

S1089-5639(98)00387-9 CCC: $15.00
Published on Web 04/11/1998

of electron acceptors on the kinetics of the emission (near band gap and deep trap) and bleach recovery. This system should affect electron-transfer processes without affecting the hole trapping dynamics.

It is well-known that electron acceptors adsorbed on the surface of the semiconductor nanoparticles quench the exciton emission by an electron-transfer process.[5,13] Methyl viologen (MV^{2+}) has been used previously as one of these quenchers.[5,14−16] It was shown that MV^{2+} can "accept" electrons on a time scale of less than 30 ps.[16] These measurements were conducted with a 30 ps laser pulse which limited the time resolution of these experiments. In the absence of MV^{2+}, electron trapping occurs by the surface traps of CdS[12] in 24−35 ps. Using a femtosecond laser, we found that electron transfer from CdS to MV^{2+} to form $MV^{\bullet+}$ took place on a time scale of 300 fs. The high-energy ($\lambda = 400$ nm) excitonic absorption of CdS nanoparticles was found to form a bleach in the lowest energy excitonic absorption region ($\lambda = 480$ nm) within ~50 fs after photoexcitation with 400 nm 100 fs laser pulses. This bleach recovered multiexponentially with the fastest component in the 30 ps time scale at low-intensity excitation condition. In the presence of surface adsorbed viologens, this recovery was accelerated to less than 7.5 ps. From this observation, we confirmed the assignment of the 30 ps to the electron trapping process in the CdS nanoparticles.[12] Since methyl viologen radical, however, was found to live much longer than the time scale of our experiment (~100 ps), the 7.5 ps excitonic band bleach recovery time cannot be due to the recombination of the electron located on $MV^{\bullet+}$ with the CdS hole, but rather must be due to the hole trapping. This conclusion was supported by another observation as discussed in the following.

Indeed, we have observed that the bleach recovery time of the optical hole in CdS nanoparticles is accompanied by a small shift (~20 meV) within a characteristic time of 2.5 ps.[12] In the present work, we found that this time constant was not affected by the adsorption of MV^{2+}. This supports the explanation that the spectral red shift results from hole trapping dynamics in the CdS nanoparticles.[12] Both the band filling and electron trapping models are discussed to explain our results which indicate that the electron is trapped much slower (30 ps) than the hole (a few picoseconds).

Materials and Method

The CdS particles were made according to the well-established procedures outlined by Henglein et al.[17] Two versions were made in order to adapt to the experimental conditions and provide stability against photodegradation. Method I dissolved 0.0252 g of $Cd(ClO_4)_2 \cdot 6H_2O$ in 300 mL of H_2O followed by injection of fresh 0.1 M sodium polyphosphate to produce 2×10^{-4} M concentration for each reactant. NaOH solutions were used to increase the pH to approximately 9.0. This mixture was then stirred under an argon stream for 30 min before a stoichiometric amount of H_2S was injected into the space above the solution with a syringe. The vessel was shaken for 2 min and stirred for 5 min followed by another 30 min of argon bubbling. Surface passivation was then achieved by raising the pH of the CdS sol to 10.5 with NaOH solution and then adding enough $Cd(ClO_4)_2$ (0.0755 g) to produce up to 300% excess Cd^{2+}. In method II the particles were prepared in the same manner but at higher concentrations for Cd^{2+}, S^{2-}, and sodium polyphosphate (1×10^{-3} M for each) and without surface passivation.

Sodium polyphosphate and $Cd(ClO_4)_2 \cdot 6H_2O$ were purchased from Aldrich. The H_2O was distilled and double deionized with a resistance ≥18 MΩ. The final concentration of CdS particles for method II was in the range 0.1−1 μM.

The amount of MV^{2+} and benzyl viologen (BV^{2+}) added was in the 100:1 ratio to CdS in order to study electron transfer to the surface adsorbed MV^{2+} only. Fluorescence decays were carried out by use of the single photon counting technique. The excitation source was the second harmonic ($\lambda = 286$ nm) of a dye laser (Spectra-Physics, model 375B) with a cavity dumper and synchronously pumped by a mode-locked Nd:YAG laser (Spectra-Physics, model 3800). The pulse width was measured on an autocorrelator and was equal to 20 ps. The detection system was a microchannel plate photomultiplier tube (Hamamatsu R1564) coupled with pulse height converter (ORTEC, model 457), providing an instrument response function of 30−40 ps (fwhm). The fluorescence decays at different wavelengths (between 500 and 820 nm) contained about 5000 counts at the maximum, and the spectral width was given by the slits of the monochromator (about 5 nm).

Transient absorption spectroscopy set up with femtosecond time resolution was constructed as follows. The 100 fs, 1 mJ/pulse, 1 kHz repetition rate was generated by a Ti−sapphire laser pumped with a 4 W argon ion laser Innova (Coherent) amplified by a regenerative amplifier (Clark MXR, Inc.) The output of the laser was split into two equal parts and was used to pump two identical quantronix OPO "TOPAS" Light Conversion Ltd. As a result, a tunable range of 300−20 000 nm excitation beam with energy up to a few 100 μJ in the middle of the tuning curve was generated in the OPO. One of the harmonics from the Ti:sapphire laser was also used as excitation source. The excitation beam travels through a computer-controlled optical delay line with a resolution of 3 μm (22 fs). A small portion of the fundamental frequency (about 40 μJ) was used to generate femtosecond continuum in a 1 mm sapphire plate. The range of the femtosecond continuum was between 400 and 1000 nm. In the case when the probe wavelength was outside this window, the output of another OPO was used as a probe beam. The probe beam was split into a signal and a reference beam. The pump and signal beams were overlapped at the sample in a way that the focus of the pump beam was slightly behind the sample. The signal and reference beams were focused into fiber optics, coupled into a monochromator, and monitored by a photodetector.

The excitation beam was modulated by an optical chopper at a frequency of 500 Hz. Two photodiodes were employed for the kinetic measurements at the exit slit of the monochromator. The excitation energy was measured with another photodiode. The photodiode signals were amplified and passed through the sample and hold circuitry and coupled to a lock-in amplifier locked at 500 Hz. Each point in the kinetic measurements at the single wavelength required 200 shots at fixed delay, and there were about 100−300 points in one delay line scan. The delay line repeatedly scanned until a reasonable signal-to-noise ratio was achieved. The typical OD change measured was in the range 0.005−0.050 OD. The cuvette sample was spun to exclude thermal effects and photodegradation of the sample.

For the spectral measurements, the exit slit of the monochromator was removed, and a CCD camera (Princeton Instruments, EUV-1024, controller ST-130) was attached in its place. The spectra of the signal and reference beam were detected and stored in the computer. The measurements of the absorbance changes for each point were determined by comparing the intensity ratio of the signal to the reference beam, with and without excitation. This was achieved by using slow shutter,

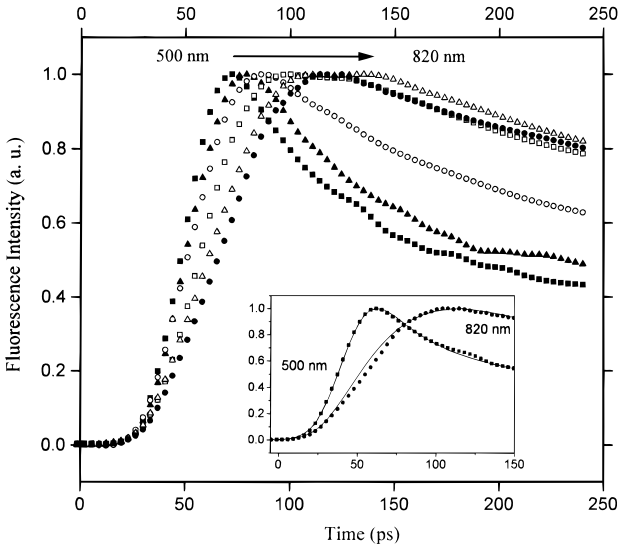

Figure 1. Fluorescence decay monitored at different wavelengths after excitation with 286 nm laser pulses: solid squares, 500 nm; solid triangles, 530 nm; open circles, 580 nm; open squares, 670 nm; open triangles, 780 nm; solid circles, 820 nm. Inset curves are measurements at 500 and 820 nm; the solid lines are fits with the parameters listed in Table 1.

TABLE 1: Dependence of the Fluorescence Rise Time on the Wavelength Obtained after Deconvolution with Apparatus Function Profile[a]

wavelength, nm	rise time, ps	wavelength, nm	rise time, ps
500	<5	670	18
530	10	780	28
580	12	820	33

[a] Excitation of CdS was with a 286 nm, 20 ps laser pulse.

blocking and unblocking the excitation beam. The data were collected until a reasonable signal-to-noise ratio was achieved. Time-resolved differences in absorbance spectra were obtained by averaging about 3000 pairs of nonexcited and excited spectra. The group velocity dispersion of the white light continuum in the optics of the probe channel and in the sample cell was compensated for by using cross-correlation data between the pump and probe pulse. For the wavelength dispersion calibration, *meso*-tetrakis(1-methyl-pyridinium-4-yl)porphyrin (H_2-TMpyP) in water solution was used because of its broad S_1-S_n transient spectrum. A typical value for the cross-correlation width was 140 fs at 500 nm.

Results

Fluorescence Emission. Steady-state emission spectra, consistent with the literature,[2,3,10,11] revealed a peak maximum centered at 500 nm for the near band-gap emission and a 580−820 nm spectral region corresponding to the deep trap emission. To obtain information about the relaxation of the charge carriers, the rise times for the fluorescence of CdS nanoparticles in the different spectral regions were recorded and are shown in Figure 1. A progressive increase in the rise time was observed with decreasing emission energy. The rise time of the luminescence, taking into account the apparatus function, changed from <5 to 33 ps on going from 500 to 820 nm (see Table 1). Previous measurements gave a rise time of the long wavelength emission as 30 ps.[2,12] The decay time of the fluorescence intensity at 500 nm is ∼35 ps, which has to be related to the 30 ps fluorescence buildup dynamics on the far red edge of the (deep trap) emission (see Table 1). Our result is in agreement with

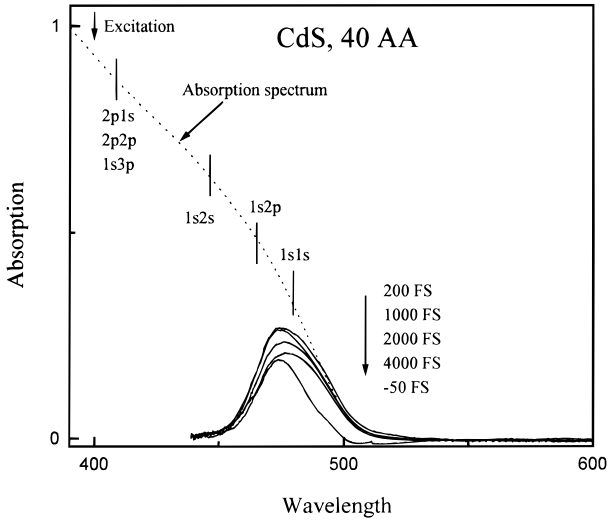

Figure 2. Time dependence of the bleach recovery (optical hole) induced in 4 nm CdS nanoparticles using 400 nm pump laser of 100 fs pulse width is represented as positive absorptions (bleaches) at 50 fs, 300 fs, 1 ps, 2 ps, and 4 ps (solid lines). The steady-state absorption spectrum is given by a dotted line, and vertical lines correspond to the calculated positions of the different excitonic states.

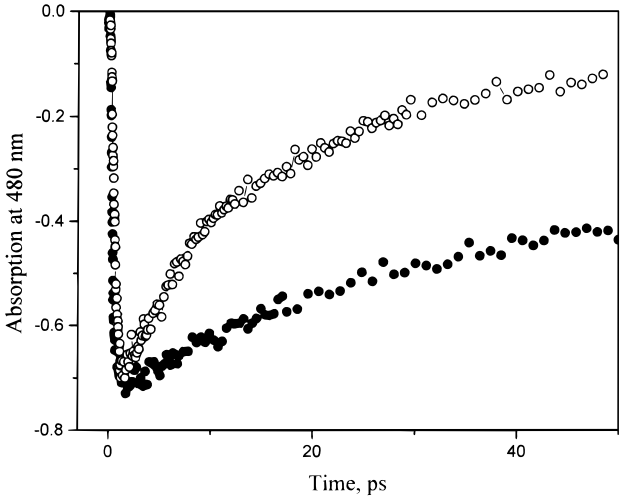

Figure 3. Kinetics of the transient bleach signal measured at 480 nm after excitation of a CdS sample (solid circles) and of CdS with MV^{2+} added (open circles) with 400 nm laser pulses of 100 fs width. The fit of the curve for CdS with MV^{2+} was carried out with three exponential curves (rise time of 200 fs, decay with 7.5 ps (0.5) and 40 ps (0.5)). The 7.5 ps decay time (bleach recovery) in samples with MV^{2+} (open circles) is much faster than the ∼30 ps decay time for CdS samples with no MV^{2+} added (solid circles).

the 20−30 ps decay obtained previously with an up-conversion technique.[12] The decay of the deep trap emission is on the microsecond time scale.

Upon the addition of MV^{2+} in a ratio of 100:1, the fluorescence intensity was completely quenched, and it was difficult to measure the emission decay. This suggests very efficient quenching of the fluorescence emission.

Transient Absorption and Bleach Recovery. The excitation of CdS nanoparticles at 400 nm led to the bleach of the absorption in the region of the lowest exciton transition to form an optical hole around 480 nm (Figure 2). The rise time of this bleach was less than 100 fs (Figure 3). The intensity of the laser pump was intentionally kept very low in order to avoid the saturation of trap states and fast Auger recombination so as to produce less than one exciton per CdS nanoparticle. The

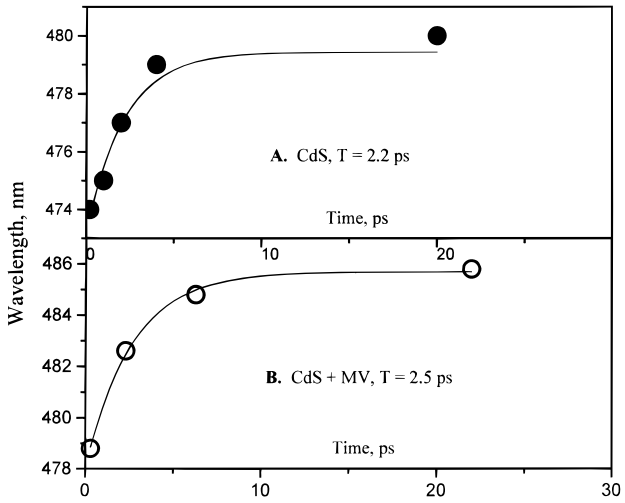

Figure 4. Time dependence of the red shift at the maximum of the optical hole (the transient bleach) formed in CdS nanocrystals (A) and that with MV^{2+} adsorbed on its surface (B). The fact that the shift occurs in 2.5 ps for both cases (i.e., is not affected by the presence of the electron acceptors) led to its assignment to hole trapping dynamics.

decay of the transient absorption at 480 nm was found to be multiexponential with 60% of the intensity having a lifetime of 35 ps (Figure 3). This lifetime is consistent with data found for CdS in glass matrix.[12] The lifetime of the slow component was outside our experimental window of 100 ps. As was shown earlier,[3] recovery of the slow component of the decay in the excitonic band ranges from a few hundred ps up to a few nanoseconds.

Figure 2 also shows that the bleaching of the optical hole is accompanied by a rapid red shift (about 5 nm) that has a characteristic time of 2.2 ps (see Figure 4). This time constant was not changed by the adsorption of the electron acceptors on the surface of the nanoparticles and thus suggests that the red-shift resulted from the hole, rather than the electron, dynamics. From an analysis of the up-converted fluorescence decay, Klimov reached a similar time scale (1 ps) for the hole relaxation dynamics.[12] Thus, as the hole is being trapped, it is possible that electrostatic interaction with the electron changes, leading to a time-dependent shift in the excitonic transition.

The addition of MV^{2+} to CdS was found to have two effects. First, at early time (less than 1 ps) a new absorption was observed (Figure 5) with a maximum at 600 nm which is characteristic of the $MV^{\bullet+}$ (radical) absorption. The rise time of the $MV^{\bullet+}$ radical absorption measured at 600 nm was 300 fs (Figure 6A). The intensity of this transient absorption remained constant for the time scale of our experiment (~100 ps).

The second effect of adding MV^{2+} was a reduction in the decay time of the excitonic transition bleach of CdS (Figure 3). The fit of the decay of the excitonic bleach recovery in the sample of CdS with MV^{2+} gave two components with lifetimes of 7.5 and 40 ps. The double-exponential decay in this case may be attributed to a large heterogeneity of the CdS particles loaded with MV^{2+}. We assign the 7.5 and 40 ps lifetimes to bleach recovery time of CdS particles with and without adsorbed MV^{2+}, respectively.

We also studied the electron-transfer process from CdS to benzyl viologen (BV^{2+}), which has a higher reduction potential than MV^{2+} by 0.1 eV. Despite this inequality in the reduction potential, it has not been possible to experimentally observe a significant difference between the electron-transfer rate constant of MV^{2+} and BV^{2+}. The rise time of $BV^{\bullet+}$ radical absorption was biexponential with a lifetime of 200 fs for the fast component and 3 ps for the long one (Figure 6B). The fast component (200 fs) could be related to the fast electron-transfer time in particles with maximum loading of CdS with BV^{2+} particles. The bleach recovery at 480 nm for CdS with BV^{2+}

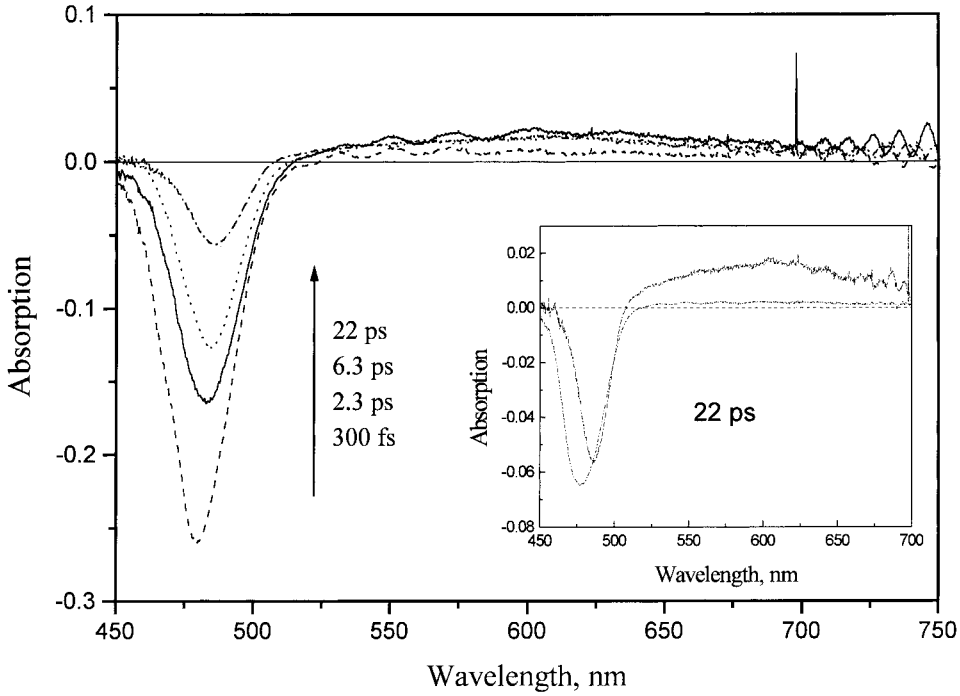

Figure 5. Time dependence of the bleach (optical hole) recovery at 480 nm for the CdS particles with MV^{2+} and the rise of the absorption of the reduced form of MV^{2+} in the 475−650 nm spectral range. The latter occurs in 300 fs (see Figure 6). Excitation at 400 nm is carried out with a laser having a pulse width of 100 fs. Delay times are 300, 2300, 6300, and 22 000 fs. The spectrum shows that an electron transfer from the CdS quantum dot to MV^{2+} is faster (300 fs) than the decay of the bleach recovery of the band gap absorption of the CdS nanoparticles (~7.5 ps). Inset: the spectrum obtained from 22 ps delay after excitation illustrates the broad $MV^{\bullet+}$ absorption (arbitrary scale) in the 500−700 nm region. For comparison, CdS with no added MV^{2+} is shown on the same time scale, but magnified 10 times.

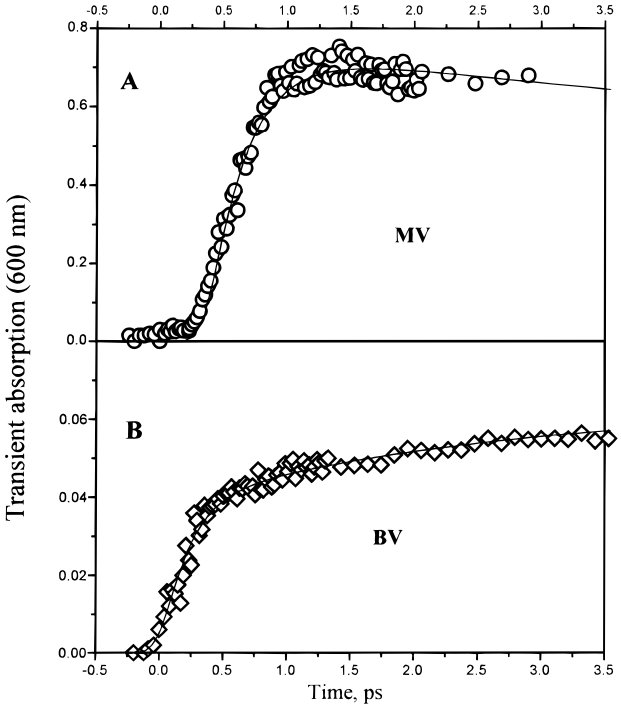

Figure 6. Kinetics of the rise of transient absorptions measured at 610 nm and excited with 400 nm laser pulses of 100 fs width for the viologen radical cations formed as a result of electron transfer from the CdS quantum dot to two different electron acceptors: MV^{2+} (A) and BV^{2+} (B). The fit of the rise has a rise time of 300 fs for (A) and a biexponential rise with rise times of 200 fs (0.55) and 3000 fs (0.45) for (B).

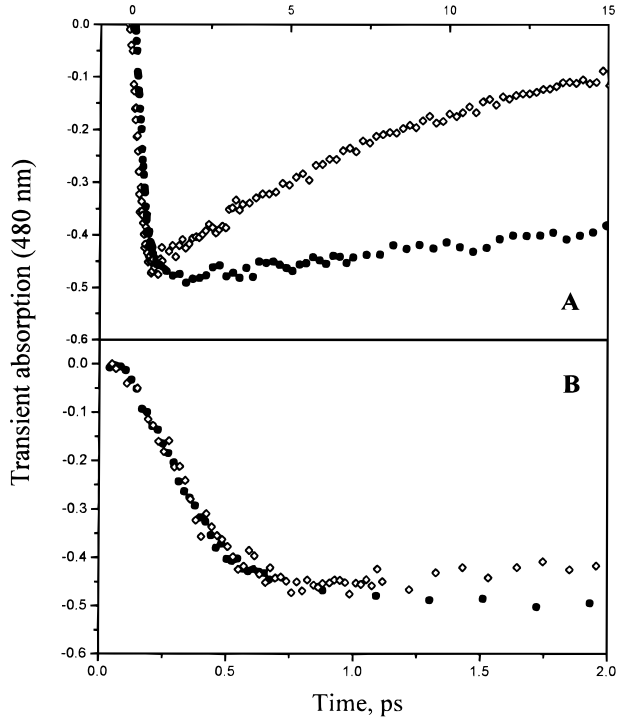

Figure 7. Decay of the bleach (optical hole) of a CdS sample with BV^{2+} added (open diamonds) at 490 nm after excitation with 400 nm laser pulses of 100 fs width. The fit corresponds to a rise time of 200 fs and decay of 9 ps. For comparison, the transient kinetics of CdS alone is also shown (solid circles). (B) is on a shorter time scale compared to (A).

has a lifetime of 9 ps (Figure 7), which is close to the 7.5 ps observed for MV^{2+} (Figure 3).

Our results may thus be summarized as follows:

1. The bleach recovery in CdS nanoparticles takes place in 30−40 ps. A red shift of the bleach maximum wavelength takes place in 2.5 ps, which was not affected by adsorption of electron acceptors. We therefore tentatively assign the 2.5 ps shift to the dynamics of the hole trapping.

2. The addition of electron acceptors accelerated the bleach recovery from 30 to 40 to <7.5 ps.

3. The reduced form of the electron acceptors ($MV^{\bullet+}$) lived much longer than the time scale of our experiment (>100 ps). We therefore conclude that the bleach recovery in the particles with electron acceptors is determined by the hole trapping process. This process should not be greatly affected by the presence of electron acceptors as it corresponds to the rate of the bleach recovery observed in CdS nanoparticles without electron acceptors (which occurred on the few picoseconds time scale).

4. The rise time of the near band edge emission is faster than the time scale of the photon counting apparatus (∼10 ps). The 30 ps time decay of the 500 nm emission is to be related to the 30 ps rise time of the deep trap emission. This 30 ps time scale is also observed in the bleach recovery dynamics of CdS nanoparticles in the absence of electron acceptors.

Discussion

For the CdS nanoparticles in solution, the 30 ps time constant was found for three processes. First, the decay of the fast component of the near band gap (shallow trap) fluorescence at 500 nm, second, the buildup of the deep trap red-shifted emission at 820 nm (Figure 1), and third the excitonic bleach recovery in the absence of viologen acceptors (Figure 3). The addition of the viologen cations to CdS nanoparticles led to the following results: (a) the rapid photoreduction of MV^{2+} and the appearance of the radical cation in 200−300 fs (Figures 5 and 6), (b) the reduction in the bleach recovery time from 30 ps in CdS NP to 7−9 ps (Figure 3), and (c) the quenching of both the near band gap and the deep trap emission.

Previously, it was shown that an electron donor molecule located on the surface of a large band gap semiconductor injects electrons, after photoexcitation, from its excited state to the conduction band of the semiconductor in ∼100 fs.[18] In this experiment, electron transfer was very efficient due to the strong overlap of the wave functions of the electron donor and conduction band (CB) states because of their high density of states. Moreover, the actual rate of electron transfer may be even higher, because the 100 fs rate constant may reflect the rate of intraband energy relaxation within the semiconductor.

The 100 fs relaxation time is consistent with the study on the dynamics of the red shift of band gap emission due to the intraband relaxation in CdS.[12] In comparison, we found evidence for an electron-transfer process from the CB of CdS to an electron acceptor molecule located at the surface in 200−300 fs. The electronic energy level of the MV^{2+} acceptor is 0.4 eV lower than the bottom of the CdS CB. One would expect the rate of electron transfer to be considerably slower than that in ref 18. The rate of 200−300 fs found in the present study suggests that the Franck−Condon factors are large due to the electron transfer to higher vibronic levels of the electron acceptor and/or the electronic coupling is reasonably large.

The combination of the time-resolved fluorescence[12] and our data on the transient absorption bleach recovery provides complementary information which explains the acceleration in the bleach recovery observed when viologen was added. Klimov et al. report that the bleach of the lowest excitonic

transition forms within ~100 fs when excitation is carried out at 400 nm. The decay of the lowest energy excitonic band occurs on a time scale of 30 ps.[12] Similar results for CdS were obtained in our measurements (Figure 3). The fluorescence dynamics of CdS is very different from that of the transient absorption. It was found that a large red shift in the fluorescence spectrum (~70 meV) occurs in a few picoseconds.[12] At the same time, the buildup of the near band gap fluorescence (2.8−2.4 eV) is observed at very early times (100 fs[12]). To explain this fact, the dominance of fluorescence by transition coupling from the extended to the localized states was proposed.[12] The localized states are presumably very closely spaced near the edge of the valence band and are populated by holes without a pump due to thermal excitation. In this case, the dynamics of near band gap emission is determined by the intraband relaxation of the carriers. The emission from deep traps, however, with energy lower than 2 eV shows a rise time of 30 ps as was found in our experiment (Figure 1). This suggests that the deep traps are populated on the time scale of 30 ps. The fast decay (~30 ps) of the fluorescence at 500 nm suggests a carrier migration from the shallow to the deep traps. The 30 ps decay time correlates with the bleach recovery time of the lowest excitonic transition from our transient absorption experiments (Figure 3). It should be mentioned that the relaxation process from higher exciton states to the band gap (lowest exciton state) occurs so rapidly that the electron hole dynamics at >30 ps are similar when excitation wavelengths at 286 (from our time-resolved fluorescence measurements) or 400 nm (from our transient absorption measurements) are used.[1c,3,5,10a,19] It is clear that the 30 ps time constant does not correspond to geminate electron−hole recombination. Two different mechanisms were proposed to explain the behavior of the excitonic band after creation of an electron−hole pair.

The first model is based on a band filling mechanism which may be used to explain the dynamics of our transient absorption data and the fluorescence measurements from ref 12. The dynamics of the bleach absorption for the excitonic transition within this model is determined by the electron and hole occupation of the states involved in transition. If one of the carriers is located on the 1s state, the allowed transition associated with this state will be bleached. Only when the slowest carrier, the electron or the hole, is trapped would the transition recover.

The second model takes into consideration the effect of the electrostatic interaction between the surface trapped electrons and the hole. The localization of the hole wave function in the vicinity of the trapped e^- is responsible for the red- shift (~50 meV) of the excitonic band and a large decrease in its oscillator strength (90%).[3] Thus in our system, the slight red shift of the bleach could be a result of the hole trapping dynamics while the bleach recovery itself results from electron trapping. At this stage it is difficult to distinguish which of the two mechanisms (band filling or electrostatic effect of surface trapping) is more important for the bleach recovery mechanism of the excitonic transition. This is due to the fact that carrier trapping in deep traps leading to the excitonic band recovery is involved in both models.

Our results on CdS without viologen as well as those of ref 12 lead to the following model. The localization of the extended exciton occurs very rapidly (in the hundreds of femtoseconds), resulting in the rise of the fast component of the near band emission (shown in Figure 1) as well as the observed slight red shift (~5 nm) in the bleach spectrum (Figure 2). The red shift is very small, only ~30 meV, and occurs on a time scale of 2.5−3 ps. Since this time was not affected by the adsorption of electron acceptors (Figure 4), this shift could be attributed to the dynamics of hole trapping. Sequentially, the electron is trapped by the deep surface traps in 30 ps. This leads to the decay of the near band gap emission, the rise of the deep trap emission, and the bleach recovery of the exciton absorption.

Electron transfer on the surface of CdS to electron acceptors, such as MV^{2+} and BV^{2+}, shows that the bleach recovery time of the excitonic absorption is decreased from 30 to 8 ps (Figure 3). The $MV^{\bullet+}$ is formed in 300 fs (Figures 5 and 6), which is a measure of the electron transfer time from the nanoparticle surface to the viologen. The fact that the intensity of the steady-state emission is quenched by the addition of the viologen without changing its kinetic profile suggests that the electron transfer process to the viologen is extremely efficient and thus competes well with the electron localization process and thus the band gap as well as the shallow near band trap emission. Since electrons in the localized state are trapped in viologen-free CdS nanoparticles by the deep traps, the addition of the electron acceptors quenches also the deep trap emission. Since the overall rate-limiting step in the bleach recovery in these CdS viologen free nanoparticles is the slow electron deep trapping process of the electrons (occurring on a 30 ps time scale), the addition of electron acceptors removes the electron in 300 fs, leaving the hole trapping process (of a few picoseconds time constant) as the rate-limiting process in the overall absorption bleach recovery. Thus, our present study of the electron-hole dynamics in CdS nanoparticles, the results on the addition of viologen electron acceptors to their surfaces, the emission results, and the bleach recovery of the spectral hole all lend strong support to the proposed model for CdS nanoparticles. Rapid exciton localization is followed by a fast hole trapping process in a few picoseconds and then a slow deep electron trapping process in ~30 ps.

Acknowledgment. The Office of Naval Research (Grant N00014-95-1-0306) and the Molecular Design Institute at Georgia Institute of Technology (Grant N00014-95-1-1116 from the Office of Naval Research) are acknowledged for their financial support of this project. S.M. thanks CNRS, France, for support that enabled her to spend six months in the LDL at Georgia Tech.

References and Notes

(1) For a review see: (a) Steigerwald, M. L.; Brus, L. E. *Acc. Chem. Res*. **1990**, *23*, 183. (b) Wang, Y.; Harron, N. *J. Phys. Chem*. **1991**, *95*, 525. (c) Wang, Y. In *Advances in Photochemistry*; Neckers, D. C., Ed.; John Wiley & Sons: New York, 1995; Vol. 19, p 179.

(2) (a) O'Neil, M.; Marohn, J.; McLendon, G. *J. Phys. Chem*. **1990**, *94*, 4356. (b) O'Neil, M.; Marohn, J.; McLendon, G. *Chem. Phys. Lett*. **1990**, *168*, 208.

(3) Wang, Y.; Suna, A.; McHugh, M.; Hilinski, E. F.; Lucas, P. A.; Johnson, R. D. *J. Chem. Phys*. **1990**, *92*, 6927.

(4) Misawa, K.; Yao, H.; Hayashi, T.; Kobayashi, T. *Chem. Phys. Lett*. **1991**, *183*, 113.

(5) Hasselbarth, A.; Eychmuller, A.; Weller, H. *Chem. Phys. Lett*. **1993**, *203*, 271.

(6) Zhang, J. Z.; O'Neil, R. H.; Roberti, T. W.; McGowen, J. L.; Evans, J. E. *Chem. Phys. Lett*. **1994**, *218*, 479.

(7) (a) Kamat, P. V.; Dimitrijevich, N. M.; Fessenden, R. W. *J. Phys. Chem*. **1987**, *91*, 396. (b) Kamat, P. V.; Ebbesen, T. W.; Dimitrijevich, N. M. *Chem. Phys. Lett*. **1989**, *157*, 384.

(8) (a) Haase, M.; Weller, H.; Henglein, A. *J. Phys. Chem*. **1988**, *92*, 4706. (b) Henglein, A. *Chem. Rev*. **1989**, *89*, 1861.

(9) (a) Rossetti, R.; Brus, L. E. *J. Phys. Chem*. **1986**, *90*, 558. (b) Chestnoy, N.; Harris, T. D.; Hull, R.; Brus, L. E. *J. Phys. Chem*. **1986**, *90*, 3393.

(10) (a) Eychmuller, A.; Hasselbarth, A.; Katsikas, L.; Weller, H. *Ber. Bunsen-Ges. Phys. Chem.* **1991**, *95*, 79. (b) Serpone, N.; Sharma, D. K.; Jamierson, M. A.; Gratzel, M.; Ramsen, J. J. *Chem. Phys. Lett.* **1985**, *115*, 473.

(11) Barzykin, A. V.; Fox, M. A. *Isr. J. Chem.* **1993**, *33*, 21.

(12) (a) Klimov, V.; Haring Bolivar, P.; Kurz, H. *Phys. Rev. B.* **1996**, *53*, 1463. (b) Klimov, V. I.; Haring-Bolivar, P.; Kurz, H.; Karavinskii, V. A. *Superlattices Microstruct.* **1996**, *20*, 395. (c) Hursche, S.; Dekorsy, T.; Klimov, V.; Kurz, H. *Appl. Phys. B.* **1996**, *62*, 3.

(13) Hagfeldt, A.; Gratzel, M. *Chem. Rev.* **1995**, *95*, 49.

(14) Dounghong, D.; Ramsden, J.; Gratzel, M. *J. Am. Chem. Soc.* **1982**, *104*, 2977.

(15) (a) Ramsen, J. J.; Gratzel, M. *Chem. Phys. Lett.* **1986**, *132*, 269. (b) Ramsen, J. J.; Gratzel, M. *J. Chem. Soc., Faraday Trans.* **1984**, *80*, 919.

(16) Nosaka, Y.; Miyama, H.; Terauchi, M.; Kobayashi, T. *J. Phys. Chem.* **1988**, *92*, 255.

(17) Spanhel, L.; Haase, M.; Weller, H.; Henglein, A. *J. Am. Chem. Soc.* **1987**, *109*, 5649.

(18) (a) Rehm, J. M.; McLendon, G. L.; Nagasawa, Y.; Yoshihaza, K. *J. Phys. Chem.* **1996**, *100*, 9577. (b) Burfeint, B.; Hannappel, T.; Storck, W.; Willig, F. *J. Phys. Chem.* **1996**, *100*, 16463.

(19) Eychmuller, A.; Hasselbarth, A.; Katsikas, L.; Weller, H. *J. Lumin.* **1991**, *48*−*49*, 745.